REFERENCES AND NOTES

1. S. J. Baserga and J. A. Steitz, in *The RNA World*, R. F. Gesteland and J. F. Atkins, Eds. (Cold Spring Harbor Laboratory Press, Cold Spring Harbor, NY, 1993), pp. 359–381.
2. S. L. Hall and R. A. Padgett, *J. Mol. Biol.* **239**, 357 (1994).
3. K. A. Montzka and J. A. Steitz, *Proc. Natl. Acad. Sci. U.S.A.* **85**, 8885 (1988).
4. K. Montzka Wassarman and J. A. Steitz, *Mol. Cell. Biol.* **12**, 1276 (1992).
5. W.-Y. Tarn, T. A. Yario, J. A. Steitz, *RNA* **1**, 644 (1995).
6. A. G. Matera and D. C. Ward, *J. Cell Biol.* **121**, 715 (1993).
7. Y. Zhuang and A. M. Weiner, *Cell* **46**, 827 (1986).
8. B. Séraphin, L. Kretzner, M. Rosbash, *EMBO J.* **7**, 2533 (1988); P. G. Siliciano and C. Guthrie, *Genes Dev.* **2**, 1258 (1988).
9. C. I. Reich, R. W. VanHoy, G. L. Porter, J. A. Wise, *Cell* **69**, 1159 (1992).
10. R. Parker, P. G. Siliciano, C. Guthrie, *ibid.* **49**, 229 (1987); Y. Zhuang and A. M. Weiner, *Genes Dev.* **3**, 1545 (1989); J. Wu and J. L. Manley, *ibid.*, p. 1553.
11. S. Kandels-Lewis and B. Séraphin, *Science* **262**, 2035 (1993); C. F. Lesser and C. Guthrie, *ibid.*, p. 1982.
12. A. J. Newman and C. Normán, *Cell* **68**, 743 (1992).
13. B. Datta and A. M. Weiner, *Nature* **352**, 821 (1991); J. Wu and J. L. Manley, *ibid.*, p. 818; H. D. Madhani and C. Guthrie, *Cell* **71**, 803 (1992); *Genes Dev.* **8**, 1071 (1994); J.-S. Sun and J. L. Manley, *ibid.* **9**, 843 (1995).
14. The human *P120* gene expression construct was prepared by PCR amplification from a genomic clone of the human *P120* gene (supplied by H. Busch) by using primers in exons 5 and 8 to generate a fragment containing nucleotides 6775 to 7632 (numbering from GenBank accession number M33132). This fragment contained exons 5 through 8 and introns E, F, and G, where intron F is the minor class intron. This fragment was cloned between the Kpn I and Hind III sites of the pCB6 mammalian expression vector [S. Andersson *et al.*, *J. Biol. Chem.* **264**, 8222 (1989)], which supplies a CMV promoter and termination and polyadenylation sites. Mutations were made either by site-directed mutagenesis of an M13 clone of this fragment followed by cloning in pCB6, or by PCR primer mutagenesis and subsequent cloning of the product in pCB6. All mutations were confirmed by sequence analysis.
15. S. L. Hall and R. A. Padgett, data not shown.
16. The human U12 snRNA expression construct was produced as described [U. Bond *et al.*, *Genes Dev.* **5**, 1709 (1991)]. Briefly, a PCR fragment of the human U12 snRNA gene (supplied by J. Steitz) (*5*) was cloned into the pUC13-U1 vector (*7*) such that the mature U12 snRNA sequences replaced the U1 snRNA sequences. U12 snRNA mutants were produced by substituting oligonucleotides containing the appropriate mutations for the PCR primer at the 5′ end of the U12 sequence and by cloning the fragments into the pUC13-U1 vector. Both the wild-type and mutant constructs have been sequenced through the 5′ and 3′ U1 snRNA gene sequences and the U12 snRNA sequences and are identical except for positions 24 and 25.
17. R. A. Padgett *et al.*, *Proc. Natl. Acad. Sci. U.S.A.* **82**, 8349 (1985); B. Ruskin, J. M. Green, M. R. Green, *Cell* **41**, 833 (1985); K. K. Nelson and M. R. Green, *Genes Dev.* **3**, 1562 (1989).
18. W.-Y. Tarn and J. A. Steitz, *Cell,* in press.
19. R. A. Padgett, M. M. Konarska, P. J. Grabowski, S. F. Hardy, P. A. Sharp, *Science* **225**, 898 (1984); B. Ruskin, A. R. Krainer, T. Maniatis, M. R. Green, *Cell* **38**, 317 (1984); C. C. Query, M. J. Moore, P. A. Sharp, *Genes Dev.* **8**, 587 (1994).
20. The pCB6-based *P120* constructs and the pUC-U12 constructs were transfected into CHO cells with the hexadimethrine bromide (Polybrene)–mediated method as described [C. Brewer and M. G. Roth, *J. Cell. Biol.* **114**, 413 (1991)]. For these experiments, 20 μg of DNA (either 10 μg of each plasmid or 10 μg of *P120* construct with 10 μg of carrier DNA) was added to a 100-mm plate containing 1.5×10^6 to 2.0×10^6 CHO cells in 5 ml of growth medium containing hexadimethrine bromide (20 μg/ml). The cells were incubated with the DNA for 6 to 8 hours followed by a 5-min shock with 5 ml of complete medium containing 30% dimethyl sulfoxide. The plates were then washed, the medium replaced, and the plates incubated for 36 to 40 hours. RNA was then extracted from the cells with the Trizol reagent (Life Technologies) following the supplier's protocol.
21. Extracted RNA was treated with 2 units of deoxyribonuclease I (Life Technologies) for 45 min at 37°C to remove residual contamination with cellular DNA. The primer for reverse transcription (CCAAGGCCAGGAGAGGCACTCGGG) was complementary to the 3′ pCB6 vector–derived sequences that are unique to the transfected *P120* minigene. The primer (150 ng) was annealed to 2 μg of RNA in reverse transcriptase buffer (BRL) by heating to 70°C and slowly cooling to 45°C. Next, deoxynucleotide triphosphates (dNTPs) and 200 units of reverse transcriptase (Superscript II, BRL) were added (for a 20-μl reaction) and incubated for 60 min at 45°C. The samples were then treated with pancreatic ribonuclease A (10 μg) for 30 min at 37°C. The resulting DNA was amplified by PCR with primers in exons 6 (CTGCCCCCTGCTGGGGAGATG) and 7 (CCCAAAATCACGCAGAATTCC) with a hot start method in 25-μl reactions containing 3 μl of the reverse transcription reaction or a control reaction from which reverse transcriptase was omitted, 2.5 pmol of each primer, 0.2 mM each dNTP, 50 mM KCl, 10 mM tris-HCl (pH 9.0), 0.1% Triton X-100, 2.5 mM $MgCl_2$, and 10 μCi of [α-^{32}P]deoxycytidine triphosphate (dCTP). PCR conditions were 94°C for 5 min followed by 30 cycles of 94°C, 57°C, and 72°C for 1 min each.
22. Supported by NIH grant RO1 GM45371. We thank J. Wei for assistance in the construction of the *P120* mutants and H. Busch, J. Steitz, A. Weiner, and M. Roth for supplying clones, vectors, and cell lines. We also thank J. Steitz and W.-Y. Tarn for communicating their results before publication.

26 December 1995; accepted 6 February 1996

Requirement for cAMP-PKA Pathway Activation by M Phase–Promoting Factor in the Transition from Mitosis to Interphase

Domenico Grieco,* Antonio Porcellini, Enrico V. Avvedimento, Max E. Gottesman

Cell cycle progression in cycling *Xenopus* egg extracts is accompanied by fluctuations in the concentration of adenosine 3′,5′-monophosphate (cAMP) and in the activity of the cAMP-dependent protein kinase (PKA). The concentration of cAMP and the activity of PKA decrease at the onset of mitosis and increase at the transition between mitosis and interphase. Blocking the activation of PKA at metaphase prevented the transition into interphase; the activity of M phase–promoting factor (MPF; the cyclin B–p34^{cdc2} complex) remained high, and mitotic cyclins were not degraded. The arrest in mitosis was reversed by the reactivation of PKA. The inhibition of protein synthesis prevented the accumulation of cyclin and the oscillations of MPF, PKA, and cAMP. Addition of recombinant nondegradable cyclin B activated p34^{cdc2} and PKA and induced the degradation of full-length cyclin B. Addition of cyclin A activated p34^{cdc2} but not PKA, nor did it induce the degradation of full-length cyclin B. These findings suggest that cyclin degradation and exit from mitosis require MPF-dependent activation of the cAMP-PKA pathway.

A rapid succession of interphase and mitotic states characterizes the early embryonic divisions of many species. The onset of mitosis is induced by activation of MPF, a highly conserved complex consisting of a kinase, p34^{cdc2}, and an activating subunit (cyclin B1 or B2) (*1*). The transition into interphase is accompanied by the destruction of MPF by ubiquitin-mediated proteolysis of the cyclin component (*2, 3*). Cyclin B synthesis plays a pivotal role in the cell cycle. It is the only protein whose synthesis is required to induce complete cycles of activation and inactivation of MPF in *Xenopus* (*4*). As cyclin accumulates and binds to p34^{cdc2}, a series of posttranslational modifications of the complex precede the activation of MPF. These reactions help to set the timing of the onset of mitosis (*5*). When p34^{cdc2} is fully activated by cyclin B, it induces cyclin degradation, whereas when it is activated by cyclin A, it does not (*6, 7*). Activation of the cyclin degradation pathway is required to complete mitosis and to allow separation of sister chromatids at anaphase (*8*).

The biochemical oscillations of the *Xenopus* embryonic cell cycle can be reproduced in cytoplasmic extracts from fertilized eggs (*4*). Neither DNA synthesis nor mitotic spindle assembly is required for the cycles

D. Grieco, Dipartimento di Biologia e Patologia Cellulare e Molecolare "L. Califano" and Centro di Endocrinologia ed Oncologia Sperimentale del CNR, II Medical School, University of Naples, Via S. Pansini 5, Naples 80131, Italy, and Institute of Cancer Research, Columbia University, 701 West 168 Street, New York, NY 10032, USA.
A. Porcellini, Dipartimento di Biologia e Patologia Molecolare e Cellulare "L. Califano" and Centro di Endocrinologia ed Oncologia Sperimentale del CNR, II Medical School, University of Naples, Via S. Pansini 5, Naples 80131, Italy.
E. V. Avvedimento, Dipartimento di Medicina Sperimentale, Medical School, University of Reggio Calabria, Via T. Campanella 5, Catanzaro, Italy.
M. E. Gottesman, Institute of Cancer Research, Columbia University, 701 West 168 Street, New York, NY 10032, USA.

*To whom correspondence should be addressed.

of MPF activation and inactivation in early frog embryos, which indicates that these biochemical oscillations are independent of the feedback controls that can affect cell cycle progression (9). The activity of PKA oscillates during the cell cycle of cycling *Xenopus* egg extracts (*10*); it is greatest at the transition from mitosis to interphase and is at a minimum at the onset of mitosis. Oscillations in the activity of PKA should reflect cycles of association and dissociation of PKA holoenzyme induced by variations in the concentration of intracellular cAMP (*11*), but regulation through the PKA inhibitor polypeptide PKI cannot be excluded (*12*).

We measured the concentration of cAMP and the activity of PKA during the cell cycle of cycling *Xenopus* egg extracts (Fig. 1) (*13*). We also monitored oscillations between interphase and mitosis by assaying the histone H1 kinase activity of MPF (*4*). MPF activity peaked when the cell cycle reached metaphase, abruptly declined at telophase, remained low during interphase, and rose again at entry into the next mitosis. A decrease in the concentration of cAMP and in the activity of PKA marked the onset of mitosis (0 to 40 min in the first cell cycle and 70 to 110 min in the second cycle). At metaphase, cAMP concentration and PKA activity rose and reached a maximum at the beginning of interphase (60 to 70 min); they fell again at the onset of the next mitosis (80 to 110 min).

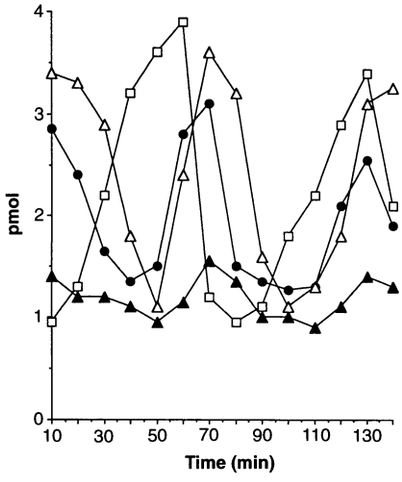

Fig. 1. Oscillations in cAMP concentration and PKA activity during the cell cycle. Kinase activity and cAMP concentration are shown as a function of the length of incubation of a cycling extract at 23°C. (□) Histone H1 kinase activity of MPF (picomoles of phosphate transferred from ATP to histone H1 per minute per 1 μl of extract at 30°C) (*4*). (△) PKA activity (picomoles of phosphate transferred from ATP to Kemptide per minute per 0.5 μl of extract at 30°C) (*13*). (▲) PKA activity in the presence of PKI (20 μM). (●) cAMP (picomoles per 15 μl of extract) (*13*). The cAMP amounts shown are the average of duplicate samples in which variability was within 12%. The oscillation patterns of MPF, PKA, and cAMP were reproducible in six independent experiments in which six independently prepared extracts were assayed, although the precise time of appearance of the peaks was extract-dependent. The activity of PKA that oscillated during the cell cycle did not exceed 10% of total PKA activity in the extracts when it was measured at saturating concentrations of cAMP in the assay reaction mixture (*10, 13*).

Activation of the ubiquitin-mediated cyclin degradation pathway is required for complete mitosis (*2, 8*). Although increased activity of MPF at metaphase is a prerequisite for cyclin degradation, the signal that initiates it is not known (*6*). We investigated whether the activation of the cAMP-PKA pathway at the transition from mitosis to interphase was required for the destruction of MPF. We blocked the increase of PKA activity at metaphase and monitored the progression of the cell cycle. We added recombinant rat PKA regulatory subunit type II β in the form of a glutathione-S-transferase (GST) fusion protein (GST-RII) (*14*) to a cycling egg extract. This fusion protein acts as a fully functional PKA regulatory subunit that binds the catalytic subunit and releases it upon cAMP addition (*15*). Addition of GST-RII after 30 min of incubation at 23°C arrested the cell cycle in mitosis in a dose-dependent manner (Fig. 2). Increasing amounts of GST-RII prolonged the inhibition of PKA activity and mitotic arrest (Fig. 2, B to D). The amount of GST-RII did not decrease during incubation, which excluded the possibility that GST-RII might stabilize cyclin B by competing for ubiquitin-mediated pro-

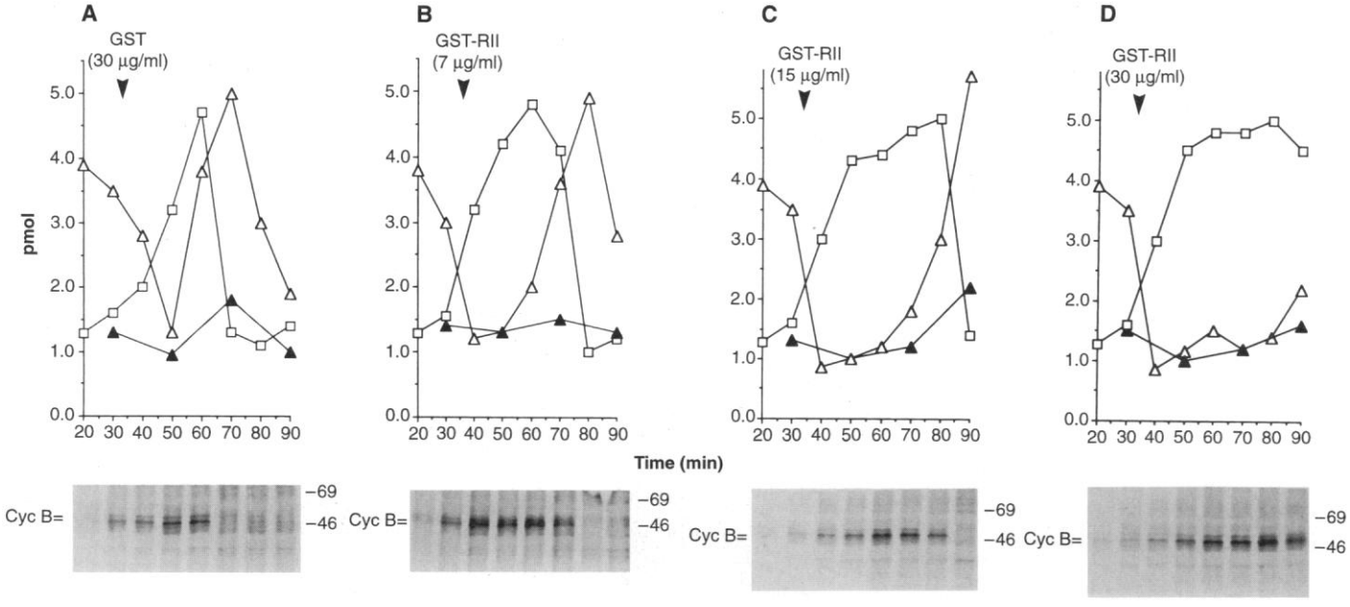

Fig. 2. Mitotic arrest induced by inhibition of PKA. Portions of a cycling extract, containing [^{35}S]methionine (400 μCi/ml), were incubated at 23°C. After 30 min of incubation, the following additions were made per milliliter of extract (5% of extract volume), and incubation was continued: (**A**) GST protein (30 μg); (**B**) GST-RII (7 μg); (**C**) GST-RII (15 μg); and (**D**) GST-RII (30 μg). From 20 to 90 min of incubation, samples were withdrawn at 10-min intervals and assayed for histone H1 kinase activity, PKA activity, and PKA activity in the presence of PKI (□, △, and ▲, respectively; units as in Fig. 1) (upper panels) or separated on a 12% polyacrylamide gel (lower panels). An autoradiograph of the gel shows the labeled proteins synthesized in the extract during the cell cycle; the positions of cyclin B are indicated. The addition of GST alone had no effect on the cell cycle. The duration of arrest for a given GST-RII concentration varied among extracts. Molecular size markers at 69 and 46 kD are shown.

teolysis (*16*). The eventual exit from mitosis in extracts treated with GST-RII may result from the accumulation of endogenously synthesized cAMP to a concentration capable of dissociating the PKA holoenzyme. The GST-RII–induced arrest was reversed when PKA holoenzyme was dissociated by addition of cAMP (Fig. 3). Mitotic arrest was induced for 20 min with GST-RII (Fig. 3, A and B), and cAMP (250 nM) was added after 50 min (Fig. 3C) or 60 min (Fig. 3D). An increase in the activity of PKA, a loss of cyclin B, and a drop in the histone H1 kinase activity of MPF immediately ensued (Fig. 3, C and D).

Cyclin B, but not the less abundant cyclin A, was visible on SDS gels of portions of extracts continuously labeled with [^{35}S]methionine (Figs. 2 and 3) (*4*). During the cell cycle, cyclin A–associated p34^{cdc2} kinase is activated earlier than is MPF, and cyclin A is degraded before cyclin B (*17*). Hence, we investigated whether cyclin A degradation also depended on PKA. To vi-

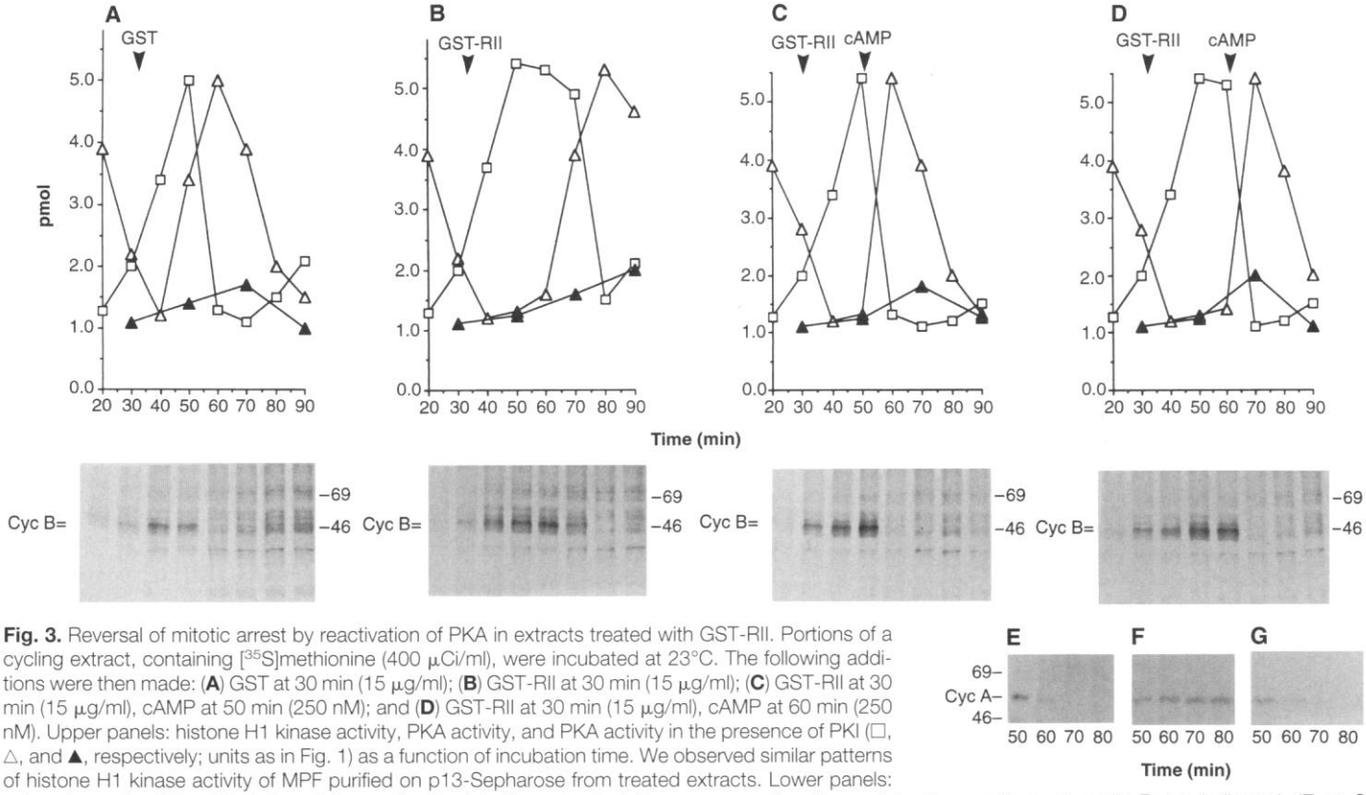

Fig. 3. Reversal of mitotic arrest by reactivation of PKA in extracts treated with GST-RII. Portions of a cycling extract, containing [^{35}S]methionine (400 μCi/ml), were incubated at 23°C. The following additions were then made: (**A**) GST at 30 min (15 μg/ml); (**B**) GST-RII at 30 min (15 μg/ml); (**C**) GST-RII at 30 min (15 μg/ml), cAMP at 50 min (250 nM); and (**D**) GST-RII at 30 min (15 μg/ml), cAMP at 60 min (250 nM). Upper panels: histone H1 kinase activity, PKA activity, and PKA activity in the presence of PKI (□, △, and ▲, respectively; units as in Fig. 1) as a function of incubation time. We observed similar patterns of histone H1 kinase activity of MPF purified on p13-Sepharose from treated extracts. Lower panels: autoradiograph of the labeled proteins synthesized in the extract at the corresponding time points; the positions of cyclin B are indicated. (**E** to **G**) Autoradiographs of [^{35}S]methionine-labeled proteins immunoprecipitated with an antibody to *Xenopus* cyclin A from extracts to which the following additions were made: (E) GST at 30 min (30 μg/ml); (F) GST-RII at 30 min (30 μg/ml); and (G) GST-RII at 30 min (30 μg/ml) and cAMP at 60 min (400 nM). The position of cyclin A is indicated. The control portion (E) had the peaks of histone H1 kinase activity and cyclin B concentration at 60 min.

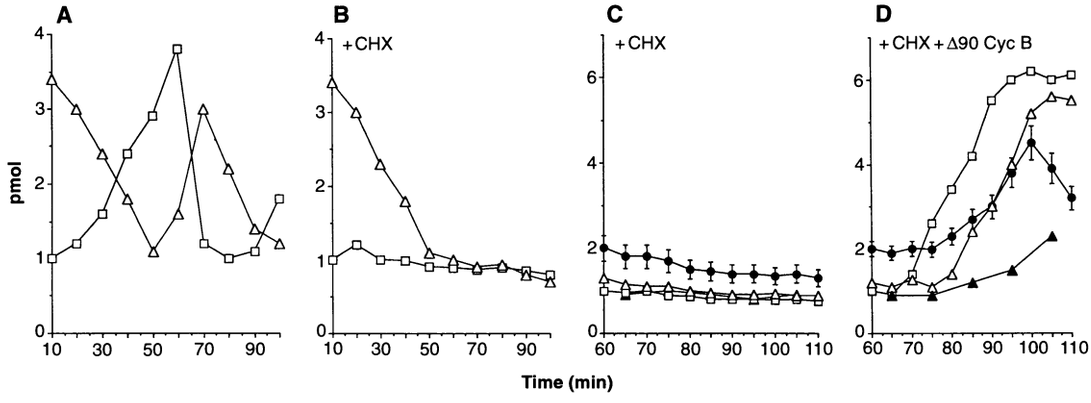

Fig. 4. Prevention of the activation of MPF and PKA by inhibition of protein synthesis, and stimulation of the cAMP-PKA pathway after MPF reactivation. (**A**) Histone H1 kinase activity and PKA activity (□ and △, respectively; units as in Fig. 1) in an incubated cycling extract. (**B**) Histone H1 kinase activity (□) and PKA activity (△) in an extract, derived from the same eggs as in (A), prepared and incubated in the presence of cycloheximide (CHX). (**C**) A portion of CHX-treated extract was incubated for 60 min at 23°C. Histone H1 kinase activity, PKA activity, and PKA activity in the presence of PKI (□, △, and ▲, respectively; units as in Fig. 1) were assayed during further incubation at 23°C, as was cAMP concentration (picomoles per 30 μl of extract; ●). (**D**) A portion of CHX-treated extract was incubated for 60 min at 23°C; then, sea urchin Δ90 cyclin B1 (15 μg/ml) was added, and the same quantities as in (C) were assayed during further incubation at 23°C. The kinetics and extent of histone H1 kinase activation were comparable to those previously observed under similar conditions (*5*). Error bars in the cAMP concentration curves indicate the variability within triplicate samples. The data are representative of three independent experiments.

sualize cyclin A, we immunoprecipitated proteins from [^{35}S]methionine-labeled extracts with an antibody to *Xenopus* cyclin A (*17*). Cyclin A was apparent after 50 min of incubation, became less abundant when the cell cycle reached metaphase at 60 min, and disappeared by 70 min (Fig. 3E; this extract had cell cycle kinetics comparable to those of the extract shown in Fig. 2A). Addition of GST-RII to the extract after 30 min of incubation inhibited the degradation of cyclin A during the next 80 min of incubation (Fig. 3F). Addition of cAMP, 30 min after the addition of GST-RII, overcame the effect of GST-RII and destabilized cyclin A (Fig. 3G).

Membrane-free sperm nuclei added to the extracts decondensed and became surrounded by nuclear membrane during the first 10 to 20 min of incubation. After 50 to 60 min, the nuclei appeared to reach metaphase and, 10 to 20 min later, underwent chromosome decondensation and nuclear envelope reassembly. Chromosome decondensation and nuclear envelope reassembly were inhibited by GST-RII addition at 30 min, and this inhibition was reversed by cAMP (*16*).

Other PKA activators such as 8-bromo-cAMP, the phosphodiesterase inhibitor isomethyl butyl xanthine, or purified PKA catalytic subunit also reversed GST-RII–induced cell cycle arrest and restored cyclin degradation (*16*). The amount of PKA activity required to restore cyclin degradation is critical. The addition of 400 nM cAMP or purified PKA catalytic subunit (4000 U/ml) (*18*) reversed the block to cyclin degradation induced by GST-RII (30 μg/ml). This treatment induced a two- to four-fold increase in the activity of PKA, similar to that observed in untreated extracts (see Fig. 1). However, greater increases in the activity of PKA (10-fold or more), caused by the addition of 50 μM cAMP or purified PKA catalytic subunit (40,000 U/ml), failed to induce cyclin degradation. This effect may be the result of nonspecific phosphorylation that occurs in the presence of nonphysiological amounts of PKA activity.

The mitotic arrest induced by GST-RII does not appear to result from a Ca^{2+}-sensitive mechanism such as the meiotic metaphase II arrest induced by cytostatic factor (CSF) (*19*). Addition of 400 μM $CaCl_2$, which inactivates CSF, did not restore cyclin degradation in extracts arrested in mitosis by GST-RII. Conversely, CSF-arrested extracts exhibited large amounts of MPF and PKA activity relative to interphase extracts, which suggested that the CSF-dependent arrest occurs after PKA activation (*16*).

The coordinated oscillations in the activities of MPF and PKA suggest a causal relation between these two functions; we

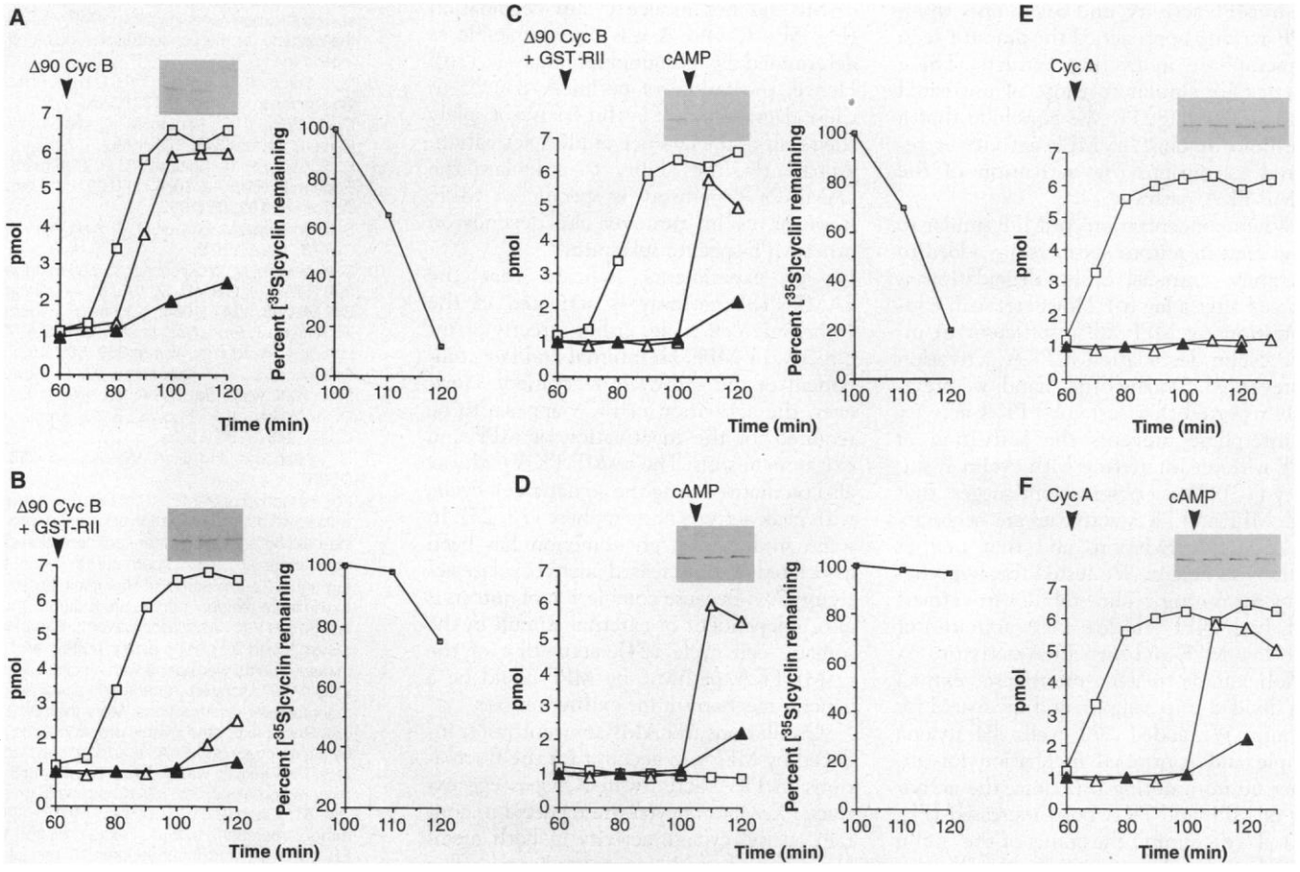

Fig. 5. Requirement of MPF, but not cyclin A–p34^{cdc2}, for activation of PKA and induction of cyclin degradation. Portions of a CHX-treated extract were incubated for 60 min at 23°C. The following reagents were then added: (**A**) Δ90 cyclin B1 (15 μg/ml); (**B**) Δ90 cyclin B1 and GST-RII (15 μg/ml); (**C**) Δ90 cyclin B1 and GST-RII (15 μg/ml), then cAMP at 100 min (250 nM); and (**D**) cAMP at 100 min (250 nM). (Left panels) Histone H1 kinase activity, PKA activity, and PKA activity in the presence of PKI (□, △, and ▲, respectively; units as in Fig. 1) during a further 60 min of incubation. Cyclin degradation was monitored by adding a reticulocyte lysate (5% of extract volume) containing [^{35}S]methionine-labeled full-length cyclin B1 after 100 min of incubation. Portions were withdrawn immediately as well as 10 and 20 min after addition of labeled cyclin (inset: an autoradiograph of the [^{35}S]methionine-labeled full-length cyclin B1 during incubation). (Right panels) Densitometric quantitation of the labeled full-length cyclin B1 remaining in the extract from the time of addition. (**E** and **F**) Portions of a CHX-treated extract were incubated for 60 min at 23°C. The following reagents were then added: (E) human cyclin A (10 μg/ml); (F) human cyclin A (10 μg/ml), then cAMP at 100 min (250 nM). The samples were assayed for histone H1 kinase activity, PKA activity, and PKA activity in the presence of PKI (□, △, and ▲, respectively) during an additional 70 min of incubation. Cyclin degradation was monitored as above.

therefore investigated whether MPF was required to induce the activation of PKA. To control the activation of MPF, we took advantage of the observation that cyclin synthesis is both necessary and sufficient to activate MPF in *Xenopus* egg extracts (*4*). We treated cycling extracts with cycloheximide to prevent cyclin synthesis (Fig. 4, A and B) and noted a steady decrease in the activities of MPF and PKA in the treated extract. To activate MPF, we incubated an extract with cycloheximide for 60 min and then added recombinant nondegradable cyclin B1 (Δ90 cyclin B1) (*2*, *20*). In the absence of Δ90 cyclin B1, the amount of cAMP and the activities of MPF and PKA remained at baseline during further incubation (Fig. 4C). Addition of Δ90 cyclin B1 potently activated MPF after a lag, as previously shown (*5*); it also stimulated PKA activity and increased the amount of cAMP (Fig. 4D). The increase in the amount of cAMP and PKA activity was delayed relative to the rise in MPF activity, and began only when MPF activity approached the amount seen at metaphase in cycling extracts. These kinetics are similar to those of untreated extracts (see Fig. 1). We conclude that a threshold amount of MPF activity is required to initiate the activation of the cAMP-PKA pathway.

When concentrations of MPF similar to those seen in mitotic extracts are added to interphase extracts, cyclin degradation is induced after a lag (*6*). However, such concentrations of MPF are insufficient to induce cyclin degradation if PKA activation is prevented. On the other hand, we previously reported that sustained PKA activity in interphase prevents the activation of MPF without interfering with cyclin B stability (*10*). These observations suggest that both MPF and PKA activities are necessary for cyclin degradation, and that neither alone is sufficient. We tested this hypothesis by measuring cyclin stability in extracts with high MPF and low PKA activities or with low MPF and high PKA activities. A cycloheximide-treated interphase extract was divided into samples and incubated for 60 min. We added Δ90 cyclin B1 to one sample and continued incubation for another 60 min; during this time, the activities of MPF and PKA both increased (Fig. 5A). To determine the status of the cyclin degradation pathway, we added [^{35}S]methionine-labeled full-length cyclin B1 (*20*) 40 min after addition of Δ90 cyclin B1. Under these conditions, the full-length cyclin was rapidly degraded (Fig. 5A). When GST-RII was added together with Δ90 cyclin B1, the degradation of the full-length cyclin B1 was inhibited as long as PKA activity remained at baseline (Fig. 5B). The inhibition of PKA and stabilization of full-length cyclin by GST-RII was reversed by cAMP (Fig. 5C). In the absence of Δ90 cyclin B1, PKA activation did not induce cyclin degradation (Fig. 5D). The full-length cyclin B1 was likewise stable in a control sample to which no additions had been made (*16*). These results indicate that neither MPF nor PKA alone can induce cyclin degradation. In the presence of large amounts of MPF, the activation of PKA appears to be required for cyclin degradation.

Cyclin A can activate p34^{cdc2} and induce maturation of prophase-arrested oocytes (*21*); however, cyclin A–p34^{cdc2} is unable to induce cyclin degradation (*7*). To determine whether cyclin A–p34^{cdc2}, like MPF, could activate PKA, we added recombinant human cyclin A to a cycloheximide-treated extract. Although histone H1 kinase activity rapidly increased, no activation of PKA was detected, and [^{35}S]methionine-labeled full-length cyclin B1 was stable under these conditions (Fig. 5E). Moreover, activation of PKA by added cAMP did not induce cyclin degradation (Fig. 5F). Cyclin A was likewise stable as determined by immunoblot analysis (*16*). Hence, the failure of cyclin A–p34^{cdc2} to cause degradation of cyclin B1 is not solely the result of the absence of PKA activation. Apparently, the ability to stimulate the cAMP-PKA pathway is specific to MPF; however, cyclin turnover also depends on other MPF-specific substrates.

Our experiments indicate that the cAMP-PKA pathway is activated in the embryonic cell cycle, either directly or indirectly, by MPF, an internal and key component of the cell cycle machinery. However, the activation of PKA appears to be required for the inactivation of MPF and exit from mitosis. The cAMP-PKA pathway also oscillates during the somatic cell cycle, with peak activity at metaphase (*22*, *23*). In some studies, this phenomenon has been associated with increased adenyl cyclase activity (*23*). Because completion of mitosis is also independent of external stimuli in the somatic cell cycle (*24*), activation of the cAMP-PKA pathway by MPF could be a general mechanism for exiting mitosis.

Oscillations in cAMP concentration induced by MPF can account for the fluctuations in PKA activity in *Xenopus* egg extracts. *Xenopus* oocytes are reported to contain adenyl cyclase activity in both membrane-bound and cytosolic forms. The former has been shown to be a target of progesterone, which induces a transient drop in cAMP concentration. The decrease in cAMP concentration appears to be required for resumption of meiosis (*25*). Whether MPF increases the intracellular concentration of cAMP by stimulating one or both adenyl cyclases, by inhibiting phosphodiesterases, or by a combination of these mechanisms is still unknown. These data, however, indicate that the control of activation-inactivation cycles of the cAMP-PKA pathway may play a critical role in regulating transitions through the cell cycle.

REFERENCES AND NOTES

1. J.-C. Labbé *et al.*, *EMBO J.* **8**, 3053 (1989); J. Gautier *et al.*, *Cell* **60**, 487 (1990); P. Nurse, *Nature* **344**, 503 (1990).
2. A. W. Murray, M. J. Solomon, M. W. Kirschner, *Nature* **339**, 280 (1989).
3. M. Glotzer, A. W. Murray, M. W. Kirschner, *ibid.* **349**, 132 (1991).
4. A. W. Murray and M. W. Kirschner, *ibid.* **339**, 275 (1989). Histone H1 kinase activity was assayed by adding 6 μl of a mixture containing histone H1 (Boehringer, 1 mg/ml), 1 mM adenosine triphosphate (ATP), and 2.5 μCi of [γ-^{32}P]ATP (Amersham, 3000 Ci/mmol) to 10 μl of extract diluted 1:50 in EB buffer [80 mM β-glycerophosphate, 15 mM $MgCl_2$, and 20 mM EGTA (pH 7.4)] and incubating for 10 min at 30°C. Histone H1 was separated in an SDS–12% polyacrylamide gel, and radioactivity was quantified by counting excised gel portions containing histone in a scintillation counter. Addition of PKI to the histone H1 kinase reaction inhibited phosphorylation by less than 5%; a similar degree of inhibition was observed in experiments in which cAMP was added to the extracts (at the concentrations indicated in the legend to Fig. 3).
5. M. J. Solomon, M. Glotzer, T. H. Lee, M. Philippe, M. W. Kirschner, *Cell* **63**, 1013 (1990).
6. M.-A. Félix, J.-C. Labbé, M. Dorée, T. Hunt, E. Karsenti, *Nature* **346**, 379 (1990).
7. F. C. Luca, E. K. Shibuya, C. E. Dohrmann, J. V. Ruderman, *EMBO J.* **10**, 4311 (1991); T. Lorca *et al.*, *J. Cell Sci.* **102**, 55 (1992).
8. S. L. Holloway, M. Glotzer, R. W. King, A. W. Murray, *Cell* **73**, 1393 (1993).
9. D. Kimelman, M. W. Kirschner, T. Scherson, *ibid.* **48**, 399 (1987); J. Gerhart, M. Wu, M. W. Kirschner, *J. Cell Biol.* **98**, 1247 (1984); K. Hara, P. Tydeman, M. W. Kirschner, *Proc. Natl. Acad. Sci. U.S.A.* **77**, 462 (1980); A. W. Murray, *Nature* **359**, 599 (1992).
10. D. Grieco, E. V. Avvedimento, M. E. Gottesman, *Proc. Natl. Acad. Sci. U.S.A.* **91**, 9896 (1994).
11. D. A. Walsh, J. P. Perkins, E. G. Krebs, *J. Biol. Chem.* **243**, 3763 (1968).
12. S. Whitehouse and D. A. Walsh, *ibid.* **258**, 3682 (1983).
13. For extraction of cAMP, 10 or 20 μl of extract was withdrawn during incubation and mixed with 1 ml of ice-cold 65% ethanol. After sedimentation of insoluble material, the supernatants were filtered through a 22-μm Acrodisc filter (Gelman Sciences) to eliminate residual particulate material and dried in a Speed Vac desiccator (Savant). Samples were resuspended in cAMP assay buffer, and cAMP measurements were done with a scintillation proximity cAMP assay kit (Amersham) according to the manufacturer's instructions. More than 80% of the cAMP was extracted by this procedure, as judged by the recovery of [^{3}H]cAMP added to extract samples. PKA activity was assayed by adding 8 μl of a mixture containing 200 μM Kemptide (Sigma), 100 μM ATP, and 2.5 μCi of [γ-^{32}P]ATP (3000 Ci/mmol, Amersham) to 4 μl of extract diluted 1:50 in EB buffer (*4*) and incubatingfor 10 min at 30°C. Where indicated, 20 μM PKI synthetic peptide (amide; Gibco) was added to the reaction mixture. Kemptide was separated in an SDS–18% polyacrylamide gel, and radioactivity was quantified by counting excised gel portions containing Kemptide in a scintillation counter.
14. The GST-RII fusion protein was made by inserting, after filling in with Klenow fragment (Promega), the Nde I fragment of the plasmid pET3a containing the rat PKA regulatory subunit type II β coding sequence (provided by C. S. Rubin) into the Sma I site of pGEX2T plasmid (Pharmacia). The GST-RII fusion

protein was prepared as described (*26*). GST-RII was stored at 4°C in 20 mM tris (pH 7.4) and 50 mM NaCl and was used within 10 days of preparation.
15. A. Porcellini, unpublished data.
16. D. Grieco, unpublished data.
17. J. Minshull, R. Golsteyn, C. S. Hill, T. Hunt, *EMBO J.* **9**, 2865 (1990). Cyclin A immunoprecipitations were done on extract samples (4 μl) diluted in EB buffer (*4*) containing 150 mM NaCl (100 μl) and cleared with protein G–agarose (Pharmacia). Antibody to *Xenopus* cyclin A (2 μl) was added to each sample, and the mixture was incubated for 6 hours at 4°C in constant rotation. Protein G–agarose was then added and incubation was continued for another hour. The beads were washed three times with 0.5 ml of EB buffer containing 150 mM NaCl. Proteins were eluted by boiling in SDS sample buffer and were separated on a 10% polyacrylamide gel. The gel was dried and autoradiographed.
18. One unit of PKA activity is equal to 1 pmol of phosphate transferred from ATP to Kemptide per minute at 30°C.
19. T. Lorca *et al.*, *Nature* **366**, 270 (1993).
20. The Δ90 cyclin B protein was a six-histidine–tagged version created by subcloning the Bgl II–Hind III fragment of sea urchin cyclin B1 cDNA into the Bam HI–Hind III sites of the plasmid pQE 10 (Qiagen). His–Δ90 cyclin B protein was prepared as follows: The insoluble material from the bacterial inclusion body was denatured with 8 M urea, 20 mM tris (pH 8), and 150 mM NaCl. The material was mixed with Ni^{2+}-agarose beads (Qiagen) and incubated for 20 min at room temperature in constant rotation. The material was applied to a column and extensively washed with 8 M urea, 20 mM tris (pH 8), and 150 mM NaCl. The His–Δ90 cyclin B protein, bound to the Ni^{2+}-agarose matrix, was renatured by exposure to a decreasing linear gradient of urea [8 M to 1 M, in 20 mM tris (pH 8) and 150 mM NaCl]. The protein was eluted with 200 mM imidazole, 20 mM tris (pH 8), and 150 mM NaCl, and dialyzed against 20 mM tris (pH 8), 150 mM NaCl, and 1 mM dithiothreitol. It was concentrated to 0.5 mg/ml with a Centricon 10 cartridge (Amicon) and stored at –70°C. Full-length sea urchin cyclin B1 was synthesized in a reticulocyte lysate (Stratagene) containing sea urchin cyclin B1 mRNA at 0.1 mg/ml and [^{35}S]methionine (>1000 Ci/mmol; Amersham) at 1 mCi/ml.
21. P. R. Clarke, D. Leiss, M. Pagano, E. Karsenti, *EMBO J.* **11**, 1751 (1992); K. Swenson, K. M. Ferrel, J. V. Ruderman, *Cell* **47**, 861 (1986).
22. M. Costa, E. W. Gerner, D. H. Russell, *J. Biol. Chem.* **251**, 3313 (1976).
23. I. H. Pastan, G. S. Johnson, W. B. Anderson, *Annu. Rev. Biochem.* **44**, 491 (1975).
24. A. B. Pardee, *Science* **246**, 603 (1989).
25. J. Finidori-Lepicard, S. Schorderet-Slatkine, J. Hanoune, E.-E. Baulieu, *Nature* **292**, 255 (1981); J. L. Maller and E. G. Krebs, *J. Biol. Chem.* **252**, 1712 (1977); S. Schorderet-Slatkine, S. Schorderet, P. Boquet, F. Godeau, E. E. Baulieu, *Cell* **15**, 1269 (1978).
26. I. Hoffman, P. R. Clarke, M. J. Marcote, E. Karsenti, G. Draetta, *EMBO J.* **12**, 53 (1993).
27. We thank T. Hunt and A. W. Murray for helpful discussions; M. Pagano, G. Draetta, I. Daar, G. F. Vande Woude, C. S. Rubin, and S. Obici for reagents; S. Scala for technical advice; and M. Berardone for artwork. Supported by Associazione Italiana per la Ricerca sul Cancro (AIRC), Consiglio Nazionale della Ricerca (Progetti Finalizzati Oncologia, Applicazioni Cliniche della Ricerca Oncologica e Ingegneria Genetica), and NIH. D.G. was supported by an AIRC fellowship.

28 August 1995; accepted 23 January 1996

Neonatal Tolerance Revisited: Turning on Newborn T Cells with Dendritic Cells

John Paul Ridge,* Ephraim J. Fuchs,† Polly Matzinger

For some time it has been thought that antigenic challenge in neonatal life is a tolerogenic rather than immunogenic event. Reexamination of the classic neonatal tolerance experiments of Billingham, Brent, and Medawar showed that tolerance is not an intrinsic property of the newborn immune system, but that the nature of the antigen-presenting cell determines whether the outcome is neonatal tolerance or immunization.

Nearly half a century ago, Burnet proposed that the function of the immune system is to distinguish self from nonself (*1*) and that self-tolerance is set early in life by the elimination of self-reactive lymphocytes (*2*, *3*). Though Burnet's group could not demonstrate such an early critical period (*4*, *5*), the paradigm was established when Medawar and colleagues (*6*) found that rodents injected at birth with hemopoietic cells from a genetically different donor were later able to accept transplants from the same donor, thereby providing support for the idea that neonatal lymphocytes are uniquely susceptible to the induction of tolerance.

In the ensuing decades, inquiries into the mechanisms involved led to two main categories of interpretation. Passive models suggest that experimental neonatal tolerance occurs by negative selection in the same way as does natural self-tolerance. Neonatal mice, having so few mature T cells, would be unable to reject the donor cells, which would therefore take up residence and circulate to the thymus to impart tolerance by deletion in the same way as do the normal cells of the recipient (*3*, *7*). Active models suggest that the newborn T cells generate predominantly suppressive, anti-idiotypic, or "deviated" T helper cell 2 (T_H2) immune responses that protect from self-rejection (*8*, *9*). However, newborn mice have occasionally been immunized to generate T_H1 responses (*10*) and, though some viruses induce tolerance if given neonatally (*11*), others immunize (*4*). These examples of neonatally induced immunity are not easily explained by either the passive or the active models of neonatal tolerance.

We analyzed the possibility that the critical components in experimental neonatal tolerance are the donor cells, not the responding T cells. Our theoretical basis was the "Danger" model (*12*), which suggests that the immune system does not discriminate between self and nonself but between dangerous and harmless entities, and that the primary distinction is made by antigen-presenting cells (APCs), which are activated to up-regulate costimulatory molecules only when induced by alarm signals from their environment [for example, by tissues undergoing stress and abnormal death or by microbial products (*12*, *13*)]. If, as suggested by "Two-Signal" models, lymphocytes are rendered tolerant by antigen recognition in the absence of costimulatory signals (*14*–*16*), then the absence of costimulation by normal, healthy peripheral tissues (*17*, *18*) should continuously induce T cell tolerance in the periphery. From this perspective, there is no need for an early period of tolerizability, and newborn T cells should have the same options as adult virgin T cells, being activated in the presence of costimulatory signals and tolerized in their absence.

Why then are newborn T cells tolerized by an injection of large numbers of spleen or bone marrow cells? We speculated that the reason might lie with the mixture of cells in the donor inocula, which contain very few professional APCs (*19*) and a large percentage of T and B cells, which cannot costimulate virgin T cells (*20*–*22*). Thus the tiny number of virgin T cells in newborn mice might easily be overwhelmed by interactions with the tolerogenic cells in the inoculum before ever having an opportunity to meet an activating APC such as a dendritic cell. We expected, however, that if we isolated the critical components of the inoculum, the neonates should become primed by an injection of dendritic cells and tolerized by the B cells.

To test this view, we injected newborn female C57BL/6 (B6) mice with B6 male cells and tested their cytotoxic T lymphocyte (CTL) responses to the male antigen H-Y. In the classic studies (*6*), the donors and recipients differed by major histocompatibility complex (MHC) antigens, to which primary responses are strong and for which the window of tolerizability is short and the induction of tolerance is a major accomplishment. To test for neonatal priming, we chose the in vitro CTL response to H-Y, which is completely dependent on prior in vivo immunization. In addition, the responses are less vigorous than those to

Section on T Cell Tolerance and Memory (Ghost Lab), Laboratory of Cellular and Molecular Immunology, National Institute of Allergy and Infectious Diseases, National Institutes of Health, Bethesda, MD 20892, USA.

*To whom correspondence should be addressed.
†Present address: Johns Hopkins Oncology Center, Baltimore, MD 21287, USA.